Competing order, Fermi surface reconstruction, and quantum oscillations in underdoped high-temperature superconductors

Ivailo Dimov, Pallab Goswami, Xun Jia, and Sudip Chakravarty

Department of Physics and Astronomy, University of California at Los Angeles, Los Angeles, California 90095, USA

We consider incommensurate order parameters for electrons on a square lattice which reduce to *d*-density wave order when the ordering wave vector **Q** is close to $\mathbf{Q}_0 = (\pi/a, \pi/a)$, *a* being the lattice spacing and describe the associated charge and current distributions within a single-harmonic approximation that conserves current to lowest order. Such incommensurate orders can arise at the mean-field level in extended Hubbard models, but the main goal here is to explore thoroughly the consequences within a Hartree-Fock approximation. We find that Fermi surface reconstruction in the underdoped regime can correctly capture the phenomenology of the recent quantum oscillation experiments that suggest incommensurate order, in particular the de Haas–van Alphen oscillations of the magnetization in high fields and very low temperatures in presumably the mixed state of these superconductors. For 10% hole doping in $YBa_2Cu_3O_{6+\delta}$, we find in addition to the main frequency around 530 T arising from the electron pocket and a hole frequency at around 1650 T, a new low frequency from a smaller hole pocket at 250 T for which there are some indications that require further investigations. The oscillation corresponding to the electron pocket will be further split due to bilayer coupling, but the splitting is sufficiently small to require more refined measurements. The truly incommensurate *d*-density wave breaks both time reversal and inversion, but the product of these two symmetry operations is preserved. The resulting Fermi surface splits into spin-up and spin-down sectors that are inversion conjugates. Each of the spin sectors results in a band structure that violates reflection symmetry, which can be determined in spin and angle-resolved photoemission spectroscopies. For those experiments such as the current photoemission experiments or the quantum oscillation measurements that cannot resolve the spin components, the bands will appear to be symmetric because of the equal mixture of the two spin sectors. There is some similarity of our results with the spiral spin-density wave order which, as pointed out by Overhauser, also breaks time reversal and inversion. Calculations corresponding to higher order commensuration produce results similar to antiphase spin stripes but appear to us to be an unlikely explanation of the experiments. The analysis of the Gorkov equation in the mixed state shows that the oscillation frequencies are unshifted from the putative normal state and the additional Dingle factor arising from the presence of the mixed state can provide a subtle distinction between the spiral spin-density wave and the *d*-density wave, although this is very difficult to establish precisely.

I. INTRODUCTION

Despite more than twenty years of intense effort, the telltale evidence of competing order parameters in the phase diagram of high-temperature cuprate superconductors remains an enigma. Other than antiferromagnetism of the undoped materials[1] and stripe order at special doping and special materials,[2] not much is truly understood. Yet, the attractive option of classifying the pseudogap as a broken-symmetry state has spurred intense interest.[3–7] Indeed, this option has the great power to unify the diverse phenomenology of these materials. We are strongly motivated by the recent quantum oscillation measurements[8–13] to address this question anew. These are the Shubnikov–de Haas (SdH) effect, the de Haas–van Alphen (dHvA) effect, and the oscillations of the Hall coefficient (R_H). The rapidly evolving experimental situation suggests, under various circumstances, evidence of commensurate and incommensurate orders. It is perhaps best at this time to explore as thoroughly as possible both kinds of order within a very general framework. Such a framework is provided by the Hartree-Fock theory.

Our basic assumption, justified when compared to experiments, is that the observed quantum oscillations in high magnetic fields and low temperatures in underdoped $YBa_2Cu_3O_{6+\delta}$ arise from the Landau levels of the quasiparticles of the Fermi liquid corresponding to the putative normal state. It is known, and shown here, that in the mixed state of many superconductors the oscillations remain unshifted in their frequencies from the normal state but exhibit increased damping. Thus, the beauty of the present experiments is that one can in principle determine the closed Fermi surfaces, through the Onsager relation that involves only the fundamental constants and the Fermi surface area, of the normal state without having to cross the upper critical field. At face value these observations have revealed some striking facts not noticed previously.[14] The most important of which is the existence of both positively and negatively charged quasiparticles in a hole doped cuprate at variance with the conventional wisdom. That these particles behave like quasiparticles in a Fermi liquid, even in the underdoped regime, which has so far been plagued with complex theoretical concerns involving the proximity to a Mott insulator,[15] is striking to say the least and should be of great value in uncovering the mystery of these enigmatic superconductors. One of us has elaborated on the striking nature of these discoveries and has explained that the root of these observations is the

Fermi surface reconstruction due to broken symmetries.[14] One of us has also elucidated the role of commensurate singlet *d*-density wave (DDW) to explain the oscillations of the Hall coefficient.[16] The Hall measurement is more telling than either SdH or dHvA because it contains the striking information regarding the sign of the charge carriers. There is evidence of the presence of electron pockets in what is really a hole doped material, which is difficult to explain without spontaneously breaking symmetries in the putative normal state, in particular by the featureless liquid of resonating valence bond theories.[17]

For a particle-hole condensate, which DDW is, the symmetry of the orbital wave function does not constrain the symmetry of the spin-wave function.[18] Triplet DDW has not yet been adequately explored and remains a subject for future work. The more recent experiments have, however, revealed some indication of an incommensurate ordering,[9] which was only briefly touched upon previously.[16,19] Here we focus on the incommensurate case.

Before we begin, it is important to state what a Hartree-Fock theory can or cannot accomplish. A Hartree-Fock theory can identify the possible broken symmetries and phases but cannot establish that such symmetries are indeed broken. The prime deficiency is the absence of all fluctuation effects, but often such deficiencies can be remedied by educated guesses. Of course, deep inside a broken-symmetry phase, critical fluctuations are absent and some of the collective modes can be physically identified from the symmetries of the order parameters. Most importantly, symmetries protect the Hartree-Fock calculations; those properties that are determined by the symmetries alone can be determined in the weak-interaction limit, where the calculations are better controlled from a suitable effective Hamiltonian. The results protected by symmetries should be at least qualitatively valid even in the strong-interaction limit.[20] However, the thermal properties in low-dimensional systems are badly predicted by the Hartree-Fock theories because fluctuations are often very important. Nonetheless, it is expected that the results at zero temperature retain a considerable degree of validity, except close to quantum critical points where quantum fluctuations become important.

When a commensurate one-dimensional (1D) charge density wave (CDW) is doped, the resulting charges may be viewed as defects in the CDW. If the interactions between them are sufficiently strong compared to their effective kinetic energy, then they will form an ordered lattice (which can be stabilized by a crossover to three dimensions if there are many 1D chains coupled together) of defects and the CDW will become incommensurate with the lattice. This can be energetically more favorable than simply doping holes into the rigid band formed in the presence of CDW order at a fixed wave vector. The reason, in the latter case, is the single-particle energy gap of the CDW. In a two-dimensional DDW state, however, there are nodes in the order parameter, so it may be more favorable for doped holes to simply go to the nodes and expand into Fermi pockets (in quasi-1D systems, however, this might not be possible, so doping must lead to incommensurability[21]). However, this cannot persist indefinitely if the DDW state is stabilized by approximate nesting since the Fermi surface would eventually move away from the nesting wave vector. Thus, incommensurate DDW order is a possibility at least over a range of doping. In this paper, we explore the phenomenology of this possibility. But it is very difficult to determine if this incommensuration happens before the commensurate gap collapses and some other order takes over. In this respect the tendency of the spin-density wave (SDW) to incommensurate is stronger because it is gapped everywhere on the Fermi surface being intrinsically a *s*-wave object.

Near half-filling, the Hubbard model, the *t*-*J* model, and generalizations of these appear to have many phases which are close in energy. Thus, small perturbations can strongly influence the competition between them. Consequently, it should not be too surprising that experiments on the cuprate superconductors have also uncovered some evidence for a cornucopia of phases, particularly on the underdoped side of the phase diagram, which appear in particular materials and for certain values of the doping level, temperature, magnetic field, etc. Depending on the interfacial energies between these phases, one way in which their competition can be resolved is through the formation of stripes[22] or other inhomogeneous patterns of microscale phase separation. Furthermore, as the cuprates are doped, their Fermi surfaces evolve away from the twofold commensurate nesting wave vector $\mathbf{Q}_0=(\pi/a,\pi/a)$, so we would expect translational symmetry-breaking order parameters to occur at incommensurate wave vectors. Hence, it would seem important for any theory of the pseudogap to incorporate the tendency toward incommensuration, which we take as further impetus to study incommensurate order parameters related to DDW order, the IC-DDW. Direct attempts to measure DDW order through neutron scattering have neither ruled it out[23,24] nor unambiguously verified its presence, but there are intriguing suggestions that it may be present.[25,26]

In Sec. II the construction of both commensurate and incommensurate order parameters are discussed. This discussion serves to motivate our principal approximations. Section III on fermiology is the heart of our paper. We begin with the calculation of the electronic spectra of a chosen IC-DDW order and deduce the corresponding areas of Fermi pockets that, through the Onsager relation, lead to the oscillation frequencies. The similarity of these results with the spiral SDW scenario is explained. Higher order commensurate DDW results are also discussed. These also turn out to be similar to the antiphase spin stripe calculations.[27] Thus, simply from a Hartree-Fock calculation it is not possible to single out a mechanism. One must invoke other considerations to distinguish between mechanisms. Next we show that interlayer coupling can lead to bilayer splitting of the areas of the electron pockets leaving the hole pockets essentially untouched. The subtleties of this result are discussed in some depth. Section IV contains a calculation of the self-energy of the quasiparticles in the mixed state patterned after the work of Stephen,[28] which we find to be by far the soundest approach despite its deficiencies. The calculation for the nodal quasiparticles of DDW is a little subtle and leads to a vortex contribution of the scattering rate that we find very reasonable. If this calculation can be better controlled, it may be possible to distinguish between the SDW and the DDW scenarios. Given the approximate nature of this calculation,

which can only yield a semiquantitative estimate, it seemed sufficient to illustrate our calculation with the commensurate case. Of course, the vortex contribution to the scattering rate is only a part of the total that also contains an impurity contribution. In the concluding section, Sec. V, we discuss our thoughts on microscopic models and whether or not incommensuration does actually occur. We also elaborate on experimental consequences of our work and point out the unresolved issues and future directions of research.

II. ORDER PARAMETERS

A. Commensurate

Before addressing the IC-DDW order parameter, let us summarize some of the features of the commensurate case.[29,30] A commensurate singlet particle-hole condensate is defined by the order parameter

$$\langle c^\dagger_{\alpha'\mathbf{k}'} c_{\alpha,\mathbf{k}} \rangle = \pm i W_\mathbf{k} \delta_{\alpha',\alpha} \delta_{\mathbf{k}',\mathbf{k}+\mathbf{Q_0}}, \tag{1}$$

where $\mathbf{Q_0} = (\pi/a, \pi/a)$. Although the right-hand side should correctly contain a factor $\pm i W_\mathbf{k}$, we will choose $i W_\mathbf{k}$ for clarity, as no confusion should arise. The electron destruction operator, $c_{\mathbf{k}\alpha}$, is indexed by the wave vector $\mathbf{k}$ and spin α; a is the lattice spacing. We say that the order is commensurate, or strictly twofold commensurate, because $2\mathbf{Q_0}$ is a reciprocal-lattice vector. The form factor $W_\mathbf{k}$ transforms nontrivially under the point group of the two-dimensional square lattice, defined by $\mathbf{R} = m a \hat{\mathbf{x}} + n a \hat{\mathbf{y}}$, where (m, n) is a set of integers positive or negative. It is related to the orbital angular momentum of the condensate. For DDW,

$$W_\mathbf{k} = \frac{W_0}{2} (\cos k_x a - \cos k_y a), \tag{2}$$

which corresponds to angular momentum $\ell = 2$ and $d_{x^2-y^2}$ symmetry. For a particle-hole condensate, the symmetry of the orbital wave function does not constrain the spin-wave function. Thus, there can also be a triplet DDW which corresponds to circulating staggered spin currents,[31] as opposed to charge currents. If we set $W(\mathbf{k})$ by a function that transforms as the identity and remove the factor i, the order parameter would correspond to the conventional CDW. Similarly, the triplet DDW is the $\ell = 2$ generalization of the conventional spin-density wave and is given by

$$\langle c^\dagger_{\alpha'\mathbf{k}'} c_{\alpha,\mathbf{k}} \rangle = i W_\mathbf{k} \hat{\mathbf{n}} \cdot \boldsymbol{\sigma}_{\alpha,\alpha'} \delta_{\mathbf{k}',\mathbf{k}+\mathbf{Q_0}}, \tag{3}$$

where $\boldsymbol{\sigma}$'s represent the Pauli matrices, and $\hat{\mathbf{n}}$ is a unit vector in the spin space. Once again, if we replace $i W_\mathbf{k}$ by unity, this order parameter is the conventional SDW.

Because W_0 is real, the order in Eq. (1) breaks time-reversal and hence represents a state with nonzero orbital current configuration. This is most easily seen in real space, where Eq. (1) can be written as (the spin indices α suppressed for clarity)

$$\langle c^\dagger_{\mathbf{R}'} c_\mathbf{R} \rangle = \pm i (-1)^{m'+n'} \frac{W_0}{2} V_{\mathbf{R}',\mathbf{R}}. \tag{4}$$

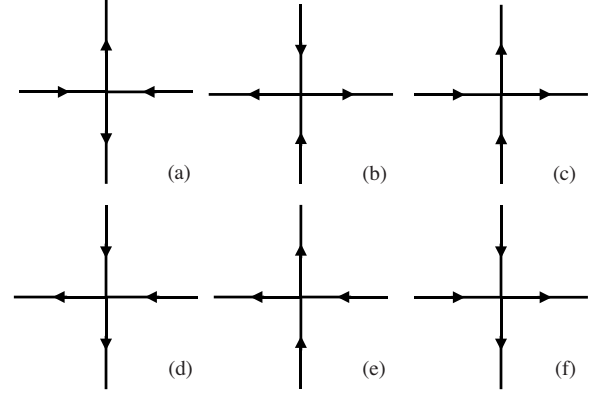The d-wave hopping amplitude factor $V_{\mathbf{R}',\mathbf{R}}$ is

FIG. 1. The six-vertex model generalization of DDW. The vertices (c)–(f) are the singlet p-wave density wave vertices. Such a model has a thermodynamic phase transition to the low-temperature DDW state but with no specific-heat anomaly.

$$V_{\mathbf{R}',\mathbf{R}} = -\delta_{\mathbf{R}',\mathbf{R}+\hat{\mathbf{x}}a} - \delta_{\mathbf{R}',\mathbf{R}-\hat{\mathbf{x}}a} + \delta_{\mathbf{R}',\mathbf{R}+\hat{\mathbf{y}}a} + \delta_{\mathbf{R}',\mathbf{R}-\hat{\mathbf{y}}a} \tag{5}$$

and also represents a current-conserving vertex centered at $\mathbf{R}$ as in Fig. 1(a).

A positive or negative sign in front of each term in Eq. (5) corresponds to current going out or in of the vertex. This analogy motivated a six-vertex description of the transition to a commensurate DDW state,[32] where in addition to the d-wave vertices in Figs. 1(a) and 1(b) one considers the effects of the p-wave vertices in Figs. 1(c)–1(f).[29] Such a description was shown to have a finite temperature phase transition without any specific-heat anomaly. As it will become evident below, one would have to include additional vertices to describe the transition to a bond-incommensurate DDW state.

B. Incommensurate

To obtain an incommensurate version of DDW order, one first notes that since it breaks the Z_2 time-reversal symmetry, one can construct anti-phase-domain walls of mutually reversed current configurations. In Fig. 2(a) we have an example of a bond-oriented domain wall. It can be written as,

$$\langle c^\dagger_{\mathbf{R}'} c_\mathbf{R} \rangle = i(-1)^{m'+n'} \frac{W_0}{2} V_{\mathbf{R}',\mathbf{R}} \times \Theta(ma) + i V^{\text{edge}}_{\mathbf{R}',\mathbf{R}}, \tag{6}$$

where

$$\Theta(x) = \begin{cases} 1, & x > 0 \\ 0, & x = 0 \\ -1, & x < 0 \end{cases} \tag{7}$$

is an overall antiphase modulation. The additional vertices $V^{\text{edge}}_{\mathbf{R}',\mathbf{R}}$ in Eq. (6) are necessary to ensure current conservation along the domain-wall boundary where the current is *half* of that in the bulk. Explicitly, they are given by the following:

$$V^{\text{edge}}_{\mathbf{R}',\mathbf{R}} = V^{\text{L}}_{\mathbf{R}',\mathbf{R}} \delta_{m,0} + V^{\text{R}}_{\mathbf{R}',\mathbf{R}} \delta_{m,1},$$

$$V^{\text{L}}_{\mathbf{R}',\mathbf{R}} = \delta_{\mathbf{R}',\mathbf{R}-\hat{\mathbf{x}}a} - \frac{1}{2}\delta_{\mathbf{R}',\mathbf{R}+\hat{\mathbf{y}}a} - \frac{1}{2}\delta_{\mathbf{R}',\mathbf{R}-\hat{\mathbf{y}}a},$$
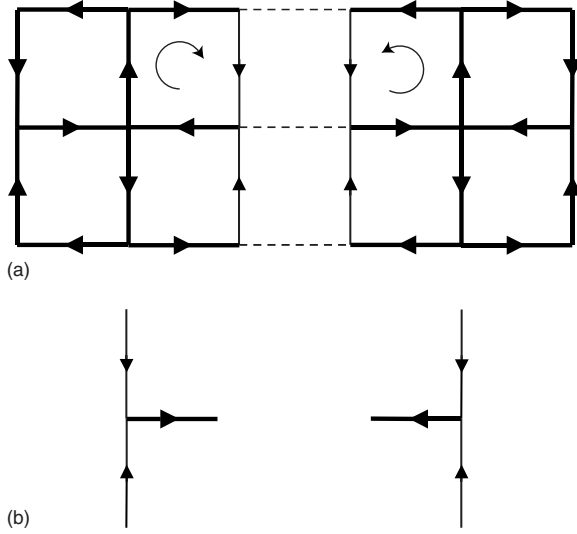
FIG. 2. (a) A bond-oriented domain wall. (b) The additional vertices ensuring current conservation at the domain boundary.

$$V^R_{\mathbf{R'},\mathbf{R}} = \delta_{\mathbf{R'},\mathbf{R}+\hat{x}a} - \frac{1}{2}\delta_{\mathbf{R'},\mathbf{R}+\hat{y}a} - \frac{1}{2}\delta_{\mathbf{R'},\mathbf{R}-\hat{y}a}, \quad (8)$$

and where $V^L_{\mathbf{R'},\mathbf{R}}$ and $V^R_{\mathbf{R'},\mathbf{R}}$ are shown in Fig. 2(b).

Note that the vertices in Eq. (8) violate both d-wave and p-wave symmetries and hence a transition to bond IC-DDW order will not be in the universality class of the six-vertex model. On the other hand, a diagonal domain wall, as in Fig. 3, does not require extra vertices, and hence the transition to diagonal IC-DDW does belong to the six-vertex model universality class.

Because the contribution of $V^{\text{edge}}_{\mathbf{R'},\mathbf{R}}$ is important only near a sharp bond-domain-wall boundary, we drop it from now on.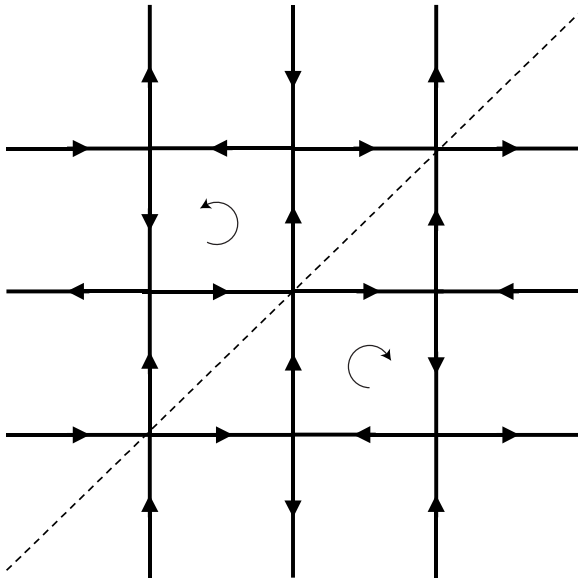 We will shortly see that at least in the single-harmonic approximation, this is justified, for it leads to current conservation up to quadratic order in the inverse domain-wall spacing. Specifically, we can consider an array of antiphase-domain walls at positions $\pm d/2, \pm 3d/2,\dots$. Because the array is periodic, we can focus on the region $-d \le ma \le d$, where due to the two domains at $\pm d/2$ the antiphase modulation $\Theta(ma)$ in Eq. (6) is replaced by

$$\theta\left(ma + \frac{d}{2}\right) - \theta\left(-ma + \frac{d}{2}\right) - 1 = \sum_{l-\text{odd}} A_l \cos\left(\frac{\pi l m a}{d}\right) \quad (9)$$

with $A_l = 4/\pi l$.

Dropping the short-range contributions $V^{\text{edge}}_{\mathbf{R'},\mathbf{R}}$ and keeping the first harmonic[33,34] $l=1$ in Eq. (9) amounts to considering an order parameter of the form

$$\langle c^\dagger_{\mathbf{R'}} c_{\mathbf{R}}\rangle = i(-1)^{m'+n'}\frac{W_0}{2}\cos(\mathbf{q}\cdot\mathbf{R})V_{\mathbf{R'},\mathbf{R}}, \quad (10)$$

where the incommensurability wave vector is proportional to the inverse domain-wall separation, so that for the bond-oriented domain in Eq. (6), $\mathbf{q}=(\pi/d,0)$. Note that we regain the commensurate case of Eq. (4) as $q\to 0$ since all domains are pushed to infinity in this limit. With the expression in Eq. (10) we can therefore analyze a continuous transition to an IC state. It remains to check that the boundary contributions $V^{\text{edge}}_{\mathbf{R'},\mathbf{R}}$ are unimportant by verifying that current is conserved at each site to quadratic order in $\mathbf{q}$.

The current along a bond $\mathbf{R}$ and $\mathbf{R}+a\hat{s}$, where $\hat{s}=\hat{x}$ or $\hat{s}=\hat{y}$, arising from the IC-DDW state, Eq. (10), is given by

$$J_{\mathbf{R},\mathbf{R}+a\hat{s}} = -\frac{W_0}{2}V_{\mathbf{R},\mathbf{R}+a\hat{s}}(-1)^{m+n}[\cos\mathbf{q}\cdot(\mathbf{R}+a\hat{s}) + \cos(\mathbf{q}\cdot\mathbf{R})]. \quad (11)$$

Therefore, the total current flowing out of a site vanishes up to quadratic order in $\mathbf{q}$.

In the momentum space, the single-harmonic expression [Eq. (10)] looks particularly simple

$$\langle c^\dagger_{\mathbf{k'}} c_{\mathbf{k}}\rangle = iW_{\mathbf{k}}[\delta_{\mathbf{k'},\mathbf{k}+\mathbf{Q}} + \delta_{\mathbf{k'},\mathbf{k}-\mathbf{Q}}]. \quad (12)$$

As the ordering wave vector $\mathbf{Q}=(\pi/a,\pi/a)+\mathbf{q}$ in Eq. (12) becomes commensurate, the above order reduces to that in Eq. (1). Moreover, because DDW is odd with respect to rotations by $\pi/2$ and transpositions about the (π,π) direction one can check that in addition to domain walls, a *checkerboard pattern* results from the following momentum-space representation:

$$\langle c^\dagger_{\mathbf{k'}} c_{\mathbf{k}}\rangle = \frac{i}{2}W_{\mathbf{k}}[\delta_{\mathbf{k'},\mathbf{k}+\mathbf{Q}} + \delta_{\mathbf{k'},\mathbf{k}-\mathbf{Q}}] - [\mathbf{Q}\to\mathcal{O}(\mathbf{Q})], \quad (13)$$

where the operation $\mathcal{O}(\mathbf{Q})$ can be either a transposition, or a rotation by $\pi/2$. Physically, the checkerboard pattern in Eq. (13) corresponds to simply superimposing two domain walls rotated by $\pi/2$ with respect to each other. In deriving Eq. (12) we have considered bond-oriented domains, but the construction is easily generalizable for the diagonal domain walls in Fig. 3.

FIG. 3. A diagonal domain wall. It can be entirely constructed from the six vertices in Fig. 1.

III. FERMIOLOGY

A. Band structure

We need to choose the band structure of the unreconstructed Fermi surface. Although this is not precisely known, it is generally accepted that it should contain at least a nearest-neighbor, a next-nearest-neighbor, and a third-neighbor matrix element in a tight-binding Hamiltonian.[35] Thus, a sufficiently general form is

$$\epsilon_{\mathbf{k}} = -2t(\cos k_x a + \cos k_y a) + 4t' \cos k_x a \cos k_y a$$
$$- 2t''(\cos 2k_x a + \cos 2k_y a). \quad (14)$$

In the past one of us has chosen[16] the parameters to be $t = 0.3$ eV, $t' = 0.3t$, and $t'' = t'/9.0$, and to be consistent we shall adhere to these, although other reasonable choices will not change our main conclusions in the least; we could even set $t'' = 0$ or set it to a larger number, such as $t'' = 0.16t$.[27] This ambiguity is understandable because the precise results are not known, either empirically or theoretically, especially in the underdoped regime. A more serious problem is to correctly reconcile the picture of the Fermi surface emerging from the quantum oscillation observations with the angle-resolved photoemission spectroscopy (ARPES).[36] Finally, we will have to choose a chemical potential, μ, to attain the carrier concentration we desire, and this we will mostly take to be about 10% of holes, simply because many quantum oscillation experiments are available for this doping level. However, we will comment on what our theory yields as the doping increases or decreases.

B. Strict incommensurability

In this subsection we address the situation when strict incommensurability holds. For example, $\mathbf{Q} = \mathbf{Q}_0 + \mathbf{q} = (\pi/a, \pi/a) - \pi(2\eta, 0)/a$, where η is not a rational number. It is of course a slight abuse of terminology to add the adjective "strict" but it dispels any possible sources of confusion. In this case each and every $\mathbf{k}$ and $\mathbf{k} + \mathbf{Q}$ correspond to a distinct point in the full Brillouin zone (BZ) of the underlying crystal lattice, and the fermion operators are similarly distinct. When necessary all sums will be carried out over the full BZ of the lattice with the conventional reciprocal-lattice vectors.

Consider now the mean-field DDW Hamiltonian given by

$$\mathcal{H} = \sum_{\mathbf{k}} \Psi_{\mathbf{k}}^{\dagger} X_{\mathbf{k}} \Psi_{\mathbf{k}}, \quad (15)$$

where

$$X_{\mathbf{k}} \equiv \begin{pmatrix} \epsilon_{\mathbf{k}} - \mu & iG_{\mathbf{k}} & 0 & 0 \\ \text{c.c.} & \epsilon_{\mathbf{k}+\mathbf{Q}} - \mu & 0 & 0 \\ 0 & 0 & \epsilon_{\mathbf{k}} - \mu & -iG'_{\mathbf{k}} \\ 0 & 0 & \text{c.c.} & \epsilon_{\mathbf{k}+\mathbf{Q}'} - \mu \end{pmatrix} \quad (16)$$

and

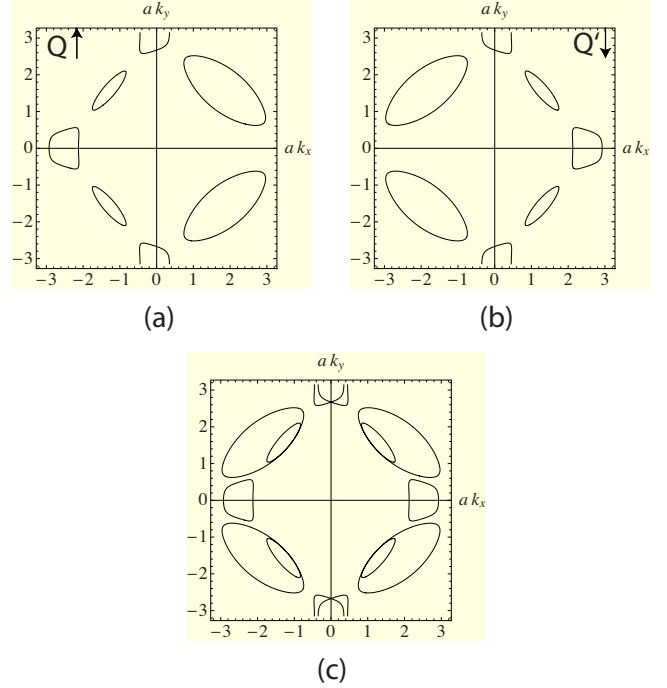$$G_{\mathbf{k}} = (W_{\mathbf{k}} - W_{\mathbf{k}+\mathbf{Q}})/2, \quad (17)$$

FIG. 4. (Color online) Reconstructed Fermi surfaces for incommensurate DDW order: (a) the up-spin case with wave vector $\mathbf{Q} = (\pi/a, \pi/a) + \mathbf{q}$; (b) the down-spin case with $\mathbf{Q}' = (\pi/a, \pi/a) - \mathbf{q}$; (c) the combined up and down-spin spectra.

$$G'_{\mathbf{k}} = (W_{\mathbf{k}} - W_{\mathbf{k}+\mathbf{Q}'})/2. \quad (18)$$

The four component spinor is $\Psi_{\mathbf{k}}^{\dagger} \equiv (c_{\mathbf{k}\uparrow}^{\dagger}, c_{\mathbf{k}+\mathbf{Q}\uparrow}^{\dagger}, c_{\mathbf{k}\downarrow}^{\dagger}, c_{\mathbf{k}+\mathbf{Q}'\downarrow}^{\dagger})$. It is useful to elaborate on this mean-field Hamiltonian. For a given wave vector $\mathbf{Q} = (\pi/a, \pi/a) + \mathbf{q}$, the inversion symmetry is broken, while the pure imaginary character of the order parameter (and the compex Hermitian character of the Hamiltonian) implies broken time-reversal symmetry. Note that the product of inversion and time reversal must be preserved as a physical requirement. Because the order parameter is a singlet in the spin space, this implies a very a simple matrix structure of the Hartree-Fock DDW Hamiltonian. The inversion conjugate of this order parameter, $\mathbf{Q}' = (\pi/a, \pi/a) - \mathbf{q}$, must belong to the down-spin sector if $\mathbf{Q}$ belongs to the up-spin sector. To further clarify the form of this Hamiltonian, note that the use of the full BZ allows us to appropriately shift the wave vectors to use identities such as

$$\sum_{\mathbf{k}} c_{\mathbf{k},\alpha}^{\dagger} c_{\mathbf{k}+\mathbf{Q},\alpha}(iG_{\mathbf{k}}) + \text{H.c.} = \sum_{\mathbf{k},\mathbf{k}'} c_{\mathbf{k}\alpha}^{\dagger} c_{\mathbf{k}'\alpha}(iW_{\mathbf{k}})[\delta_{\mathbf{k}',\mathbf{k}+\mathbf{Q}}$$
$$+ \delta_{\mathbf{k}',\mathbf{k}-\mathbf{Q}}] + \text{H.c.} \quad (19)$$

for any given spin direction α.

The Fermi surfaces obtained from the spectra of Eq. (16) are shown in Fig. 4. The pockets proximate to $(\pm\pi/a, \pm\pi/a)/2$ are hole pockets while those close to $(\pi/a, 0)$ and its symmetry equivalents are electron pockets. To obtain this figure we have chosen $W_0 = 0.112$ eV, $\eta = 0.09$,[37] $\mu = -0.256$ eV, and $n_h \approx 10\%$. The corresponding dHvA frequencies determined by the Onsager relation

$$F = \frac{\hbar c}{2\pi e} A(\epsilon_F), \tag{20}$$

where $A(\epsilon_F)$ is the cross sectional area of a closed Fermi surface, are $F_1 = 526$ T (electron pocket), $F_2 = 1670$ T (large hole pocket), and $F_3 = 250$ T (small hole pocket). We have chosen the parameters to fit the data,[9] but the existence and frequency of the small hole pocket is a prediction for which there appears to be very preliminary indications requiring further investigations and confirmation.[9]

It is important to specify how we arrive at the total hole doping of 10%. Fermi surface is a topological invariant.[38] Even when quasiparticles behave anomalously, as in one-dimensional electronic systems, this surface is still defined by the same topological invariant. A break up of this surface, termed reconstruction, requires a global deformation in the topological sense, most likely a macroscopic broken symmetry. The key here is Luttinger's sum rule. The most general form of this sum rule states that the particle density is twice (for two spin directions) the volume of the wave vector space in d dimensions divided by $(2\pi)^d$ over which the real part of the single-particle Green's function at the Fermi energy is positive, which applies even to Mott insulators.[39] This is easily applied here. There is one big hole pocket for a given spin direction within the *reconstructed* BZ. Considering the two spin directions producing identical pockets but reflected with respect to each other, the big hole pockets correspond to a fraction of carriers, x_{bh}, to be

$$x_{bh} = 2\frac{A_{bh}(\epsilon_F)}{(2\pi/a)^2}, \tag{21}$$

in terms of carriers per Cu. Here $A_{bh}(\epsilon_F)$ is the area of a big hole pocket. Note that the normalization in Eq. (23) is with respect to the area of the *unreconstructed* BZ. Similarly, there is only one-electron pocket in the *reconstructed* BZ and therefore the fraction of carriers, x_e, is, considering both spin partners,

$$x_e = 2\frac{A_e(\epsilon_F)}{(2\pi/a)^2}. \tag{22}$$

But there is also one small hole pocket per *reconstructed* BZ and therefore

$$x_{sh} = 2\frac{A_{sh}(\epsilon_F)}{(2\pi/a)^2}. \tag{23}$$

The hole doping, n_h, is

$$n_h = x_{bh} + x_{sh} - x_e. \tag{24}$$

It is important to compare the DDW case with the spiral SDW case. The mean-field potential, V_{spiral}, is

$$V_{spiral} = V_0[S_x \cos(\mathbf{Q} \cdot \mathbf{R}) + S_y \sin(\mathbf{Q} \cdot \mathbf{R})], \tag{25}$$

where S_x and S_y are the conventional spin half operators. As pointed out by Overhauser,[40,41] this interaction Hamiltonian breaks time reversal and inversion. It immediately follows that the mean-field Hamiltonian matrix for the spiral SDW is

$$Y_{\mathbf{k}} = \begin{pmatrix} \epsilon_{\mathbf{k}} - \mu & \Delta & 0 & 0 \\ \Delta & \epsilon_{\mathbf{k}+\mathbf{Q}} - \mu & 0 & 0 \\ 0 & 0 & \epsilon_{\mathbf{k}} - \mu & \Delta \\ 0 & 0 & \Delta & \epsilon_{\mathbf{k}+\mathbf{Q}'} - \mu \end{pmatrix}, \tag{26}$$

where the four component spinor is $\Phi_{\mathbf{k}}^{\dagger} \equiv (c_{\mathbf{k}\uparrow}^{\dagger}, c_{\mathbf{k}+\mathbf{Q}\downarrow}^{\dagger}, c_{\mathbf{k}\downarrow}^{\dagger}, c_{\mathbf{k}+\mathbf{Q}'\uparrow}^{\dagger})$. Here, Δ, the spiral SDW gap parameter is of course real. But it is trivial to see that the eigenvalue structure is identical to the IC-DDW because both inversion and time reversal are broken. In contrast to IC-DDW, however, the up and down sectors are mixed instead, as it should be, because DDW is a singlet in spin space, while SDW is a triplet, bearing in mind that both condensates are in the particle-hole channel. We can redefine, however, the spinors, such as

$$\begin{pmatrix} d_{\mathbf{k},\alpha} \\ d_{\mathbf{k}+\mathbf{Q},\alpha} \end{pmatrix} = \begin{pmatrix} c_{\mathbf{k},\alpha} \\ i\epsilon_{\alpha\beta}c_{\mathbf{k}+\mathbf{Q},\beta} \end{pmatrix}, \tag{27}$$

similarly for $\mathbf{Q} \to \mathbf{Q}'$. The antisymmetric tensor $\epsilon_{\alpha\beta}$ is defined by $\epsilon_{11} \equiv \epsilon_{\uparrow\uparrow} = \epsilon_{22} \equiv \epsilon_{\downarrow\downarrow} = 0$, $\epsilon_{12} \equiv \epsilon_{\uparrow\downarrow} = 1$, and $\epsilon_{21} \equiv \epsilon_{\downarrow\uparrow} = -1$. With the redefined spinors the Hamiltonian matrix is now

$$Y'_{\mathbf{k}} = \begin{pmatrix} \epsilon_{\mathbf{k}} - \mu & i\Delta & 0 & 0 \\ -i\Delta & \epsilon_{\mathbf{k}+\mathbf{Q}} - \mu & 0 & 0 \\ 0 & 0 & \epsilon_{\mathbf{k}} - \mu & -i\Delta \\ 0 & 0 & i\Delta & \epsilon_{\mathbf{k}+\mathbf{Q}'} - \mu \end{pmatrix}, \tag{28}$$

which closely resembles Eq. (16). The transformation clearly leaves the anticommutation rules unchanged.

The Fermi surfaces resulting from Eq. (26) are essentially indistinguishable from Fig. 4. This is despite the fact that the SDW order parameter is a triplet and is gapped, separating the valence band and the conduction band over the entire Fermi surface, in contrast to the DDW order parameter. This is unfortunate because from dHvA frequencies, there is no way of telling if they arise from an incommensurate spiral SDW or an incommensurate DDW; one must invoke other considerations. In constructing this Fermi surface, we have chosen the following parameters: $\Delta = 0.08$ eV, $\eta = 0.08$, $\mu = -0.27$ eV, and $n_h \approx 10\%$. The corresponding dHvA frequencies are $F_1 = 533$ T (electron pocket), $F_2 = 1667$ T (large hole pocket), and $F_3 = 274$ T (small hole pocket). We suspect that a more diligent optimization of these parameters could be performed but it will not change the main observations.

C. Higher order commensurability

As an example, consider higher order incommensuration of $\mathbf{Q} = \mathbf{Q}_0 - \frac{\pi}{a}(2 \times \frac{1}{8}, 0) = \frac{\pi}{a}(\frac{3}{4}, 1)$. With the eight-component spinor defined by $\chi_{\mathbf{k}}^{\dagger} = (c_{\mathbf{k},\alpha}^{\dagger}, c_{\mathbf{k}+\mathbf{Q},\alpha}^{\dagger}, c_{\mathbf{k}+2\mathbf{Q},\alpha}^{\dagger}, \dots c_{\mathbf{k}+7\mathbf{Q}}^{\dagger})$, the Hamiltonian can be written as

$$\mathcal{H} = \sum_{\mathbf{k},\alpha} \chi_{\mathbf{k}\alpha}^{\dagger} Z_{\mathbf{k},\alpha} \chi_{\mathbf{k}\alpha}. \tag{29}$$

Now the up and down-spin sector eigenvalues merely duplicate each other, and we can consider simply one of them

$$Z_{\mathbf{k}} = \begin{pmatrix} \epsilon_{\mathbf{k}} - \mu & iG_{\mathbf{k}} & 0 & 0 & 0 & 0 & 0 & -iG_{\mathbf{k}+7\mathbf{Q}} \\ \text{c.c} & \epsilon_{\mathbf{k}+\mathbf{Q}} - \mu & iG_{\mathbf{k}+\mathbf{Q}} & 0 & 0 & 0 & 0 & 0 \\ 0 & \text{c.c} & \epsilon_{\mathbf{k}+2\mathbf{Q}} - \mu & iG_{\mathbf{k}+2\mathbf{Q}} & 0 & 0 & 0 & 0 \\ 0 & 0 & \text{c.c} & \epsilon_{\mathbf{k}+3\mathbf{Q}} - \mu & iG_{\mathbf{k}+3\mathbf{Q}} & 0 & 0 & 0 \\ 0 & 0 & 0 & \text{c.c} & \epsilon_{\mathbf{k}+4\mathbf{Q}} - \mu & iG_{\mathbf{k}+4\mathbf{Q}} & 0 & 0 \\ 0 & 0 & 0 & 0 & \text{c.c} & \epsilon_{\mathbf{k}+5\mathbf{Q}} - \mu & iG_{\mathbf{k}+5\mathbf{Q}} & 0 \\ 0 & 0 & 0 & 0 & 0 & \text{c.c} & \epsilon_{\mathbf{k}+6\mathbf{Q}} - \mu & iG_{\mathbf{k}+6\mathbf{Q}} \\ iG_{\mathbf{k}+7\mathbf{Q}} & 0 & 0 & 0 & 0 & 0 & \text{c.c} & \epsilon_{\mathbf{k}+7\mathbf{Q}} - \mu \end{pmatrix}. \tag{30}$$

In the real space, we have

$$\langle c_{\mathbf{R}'}^{\dagger} c_{\mathbf{R}} \rangle = \frac{1}{N} \sum_{\mathbf{k}'\mathbf{k}} \langle c_{\mathbf{k}'}^{\dagger} c_{\mathbf{k}} \rangle \exp[-i(\mathbf{k}' \cdot \mathbf{R}' - \mathbf{k} \cdot \mathbf{R})]$$

$$= \pm \frac{i}{N} \sum_{\mathbf{k}} G_{\mathbf{k}} \exp[i\mathbf{k} \cdot (\mathbf{R} - \mathbf{R}')] \exp[-i\mathbf{Q} \cdot \mathbf{R}']$$

$$= \pm \frac{iW_0}{2} (-1)^{n'+m'} (\tilde{V}_{\mathbf{R}',\mathbf{R}} + i\tilde{U}_{\mathbf{R}',\mathbf{R}}), \tag{31}$$

where $\mathbf{R}' = (m'a, n'a)$, and $\tilde{V}_{\mathbf{R}',\mathbf{R}}$ and $\tilde{U}_{\mathbf{R}',\mathbf{R}}$ are of the form:[42]

$$\tilde{V}_{\mathbf{R}',\mathbf{R}} = \left[\frac{1 + \cos 2\pi\eta}{2} (\delta_{\mathbf{R}',\mathbf{R}+a\hat{\mathbf{x}}} + \delta_{\mathbf{R}',\mathbf{R}-a\hat{\mathbf{x}}}) \right.$$
$$\left. - (\delta_{\mathbf{R}',\mathbf{R}+a\hat{\mathbf{y}}} + \delta_{\mathbf{R}',\mathbf{R}-a\hat{\mathbf{y}}}) \right] \cos 2m'\pi\eta$$
$$+ \frac{\sin 2\pi\eta \sin 2m'\pi\eta}{2} (\delta_{\mathbf{R}',\mathbf{R}+a\hat{\mathbf{x}}} - \delta_{\mathbf{R}',\mathbf{R}-a\hat{\mathbf{x}}}),$$

$$\tilde{U}_{\mathbf{R}',\mathbf{R}} = -\left[\frac{1 + \cos 2\pi\eta}{2} (\delta_{\mathbf{R}',\mathbf{R}+a\hat{\mathbf{x}}} + \delta_{\mathbf{R}',\mathbf{R}-a\hat{\mathbf{x}}}) \right.$$
$$\left. - (\delta_{\mathbf{R}',\mathbf{R}+a\hat{\mathbf{y}}} + \delta_{\mathbf{R}',\mathbf{R}-a\hat{\mathbf{y}}}) \right] \sin 2m'\pi\eta$$
$$+ \frac{\sin 2\pi\eta \cos 2m'\pi\eta}{2} (\delta_{\mathbf{R}',\mathbf{R}+a\hat{\mathbf{x}}} - \delta_{\mathbf{R}',\mathbf{R}-a\hat{\mathbf{x}}}). \tag{32}$$

We compute the current pattern from

$$J_{\mathbf{R}',\mathbf{R}} = i[\langle c_{\mathbf{R}'}^{\dagger} c_{\mathbf{R}} \rangle - \langle c_{\mathbf{R}}^{\dagger} c_{\mathbf{R}'} \rangle] = -W_0 (-1)^{n'+m'} \tilde{V}_{\mathbf{R}',\mathbf{R}}. \tag{33}$$

As an example, the current pattern with $\eta = 1/8$ is drawn in Fig. 5. The relative amplitudes of currents on bonds are labeled by different arrows. Because $Q_y = \pi/a$, the currents on a vertical slice have same amplitudes but alternating directions. $Q_x = \pi/a - 2\pi\eta/a = 3\pi/4a$ results in a modulation of a period of eight lattice spacing along the horizontal direction.

From $\Sigma_{\mathbf{k} \in BZ} G_{\mathbf{k}} = 0$, it follows that $\langle c_{\mathbf{R}}^{\dagger} c_{\mathbf{R}} \rangle = 0$. This result is in disagreement with Ref. 42, where the sum was incorrectly performed over the reduced Brillouin zone (RBZ). Namely there is no site charge modulation in the higher order commensurate d-density wave state. However, note that $\tilde{U}_{\mathbf{R}',\mathbf{R}} \neq 0$ for $\mathbf{R} \neq \mathbf{R}'$, and there are bond charge modulations.

The Fermi surface corresponding to the spectra of Eq. (30) is shown in Fig. 6. It is not essentially different from the mean-field theory of 1/8 magnetic antiphase stripe order.[27] This higher order commensuration generically produces complicated Fermi surfaces, involving open orbits, hole pockets, and electron pockets. However, it is difficult to satisfy simultaneously the constraints of the Luttinger sum rule, the periodicity of the oscillations, and the negative sign of the Hall coefficient; see, however, Ref. 43. It is not clear how this picture can be consistent with experiments, unless disorder, fluctuations, or magnetic breakdown[44] conspire delicately to reproduce the experimental observations, which of course cannot be ruled out. We shall not pursue this approach further.

D. Interlayer tunneling and bilayer splitting

Bilayer coupling, $t_{\perp}(\mathbf{k})$, in YBCO is parametrized in terms of a momentum-conserving tunneling matrix element. For tetragonal structure it is[35,45]

$$t_{\perp}(\mathbf{k}) = \frac{t_{\perp}}{4} [\cos(k_x a) - \cos(k_y a)]^2, \tag{34}$$

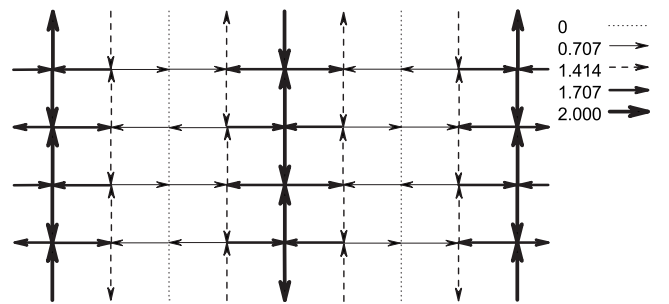where a is the lattice spacing. The tunneling Hamiltonian H_{12} is given by

FIG. 5. Current pattern for $\mathbf{Q} = (\frac{3\pi}{4a}, \frac{\pi}{a})$. The relative magnitudes of the currents are depicted by the arrows in the legend. Note the antiphase-domain wall structure.
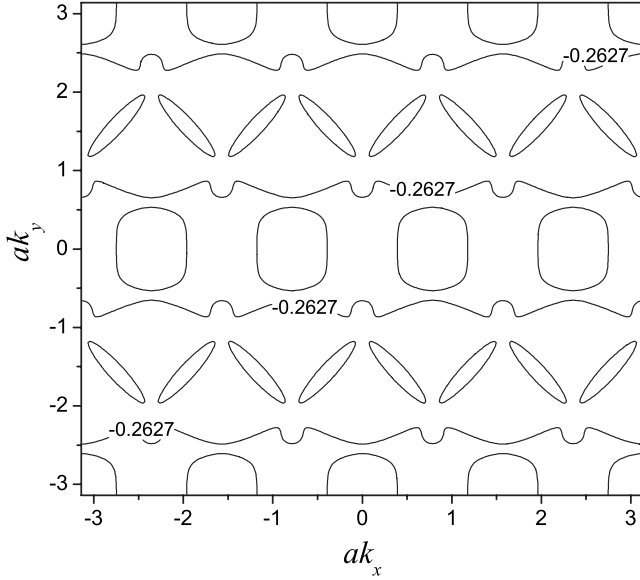
FIG. 6. Reconstructed Fermi surfaces for a plausible high order commensurate DDW with $\mathbf{Q}=\frac{\pi}{a}(\frac{3}{4},1)$ and $W_0=0.0825$ eV. There are electron pockets, hole pockets, and open orbits. Note that the figure is depicted in the extended BZ for clarity.

$$H_{12} = \sum_{\mathbf{k},\alpha} t_{\perp}(\mathbf{k})(c_{\mathbf{k},\alpha}^{\dagger(1)} c_{\mathbf{k},\alpha}^{(2)} + 1 \leftrightarrow 2). \tag{35}$$

The superscripts on the fermion operators refer to the layer index. For simplicity consider first the commensurate case. The Hartree-Fock approximation, $H_0 = H_1 + H_2$ can be written as the effective DDW Hamiltonians

$$H_0 = \sum_{\mathbf{k}\in\text{RBZ},\alpha} (\epsilon_{\mathbf{k}} c_{\mathbf{k},\alpha}^{\dagger(1)} c_{\mathbf{k},\alpha}^{(1)} + \epsilon_{\mathbf{k}+\mathbf{Q}_0} c_{\mathbf{k}+\mathbf{Q}_0,\alpha}^{\dagger(1)} c_{\mathbf{k}+\mathbf{Q}_0,\alpha}^{(1)})$$
$$+ \sum_{\mathbf{k}\in\text{RBZ},\alpha} (iW_{\mathbf{k}} c_{\mathbf{k}\alpha}^{\dagger(1)} c_{\mathbf{k}+\mathbf{Q}_0,\alpha}^{(1)} + \text{H.c.}) + (1 \leftrightarrow 2). \tag{36}$$

The reduced Brillouin zone is bounded by $k_y \pm k_x = \pm \pi/a$. With the choice of the quadratic Hamiltonian H_0 in Eq. (36), it can be easily diagonalized along with H_{12}. This is a first-order degenerate perturbation theory. Because $t_{\perp}$ will turn out to be so small, we do not expect a large correction.

At each wave vector k in the RBZ, we need to diagonalize a 4×4 matrix to extract the energy eigenvalues. This matrix is[19]

$$\mathbb{H} = \begin{pmatrix} \epsilon_{\mathbf{k}} & iW_{\mathbf{k}} & t_{\perp}(\mathbf{k}) & 0 \\ -iW_{\mathbf{k}} & \epsilon_{\mathbf{k}+\mathbf{Q}_0} & 0 & t_{\perp}(\mathbf{k}+\mathbf{Q}_0) \\ t_{\perp}(\mathbf{k}) & 0 & \epsilon_{\mathbf{k}} & iW_{\mathbf{k}} \\ 0 & t_{\perp}(\mathbf{k}+\mathbf{Q}_0) & -iW_{\mathbf{k}} & \epsilon_{\mathbf{k}+\mathbf{Q}_0} \end{pmatrix}. \tag{37}$$

From $t_{\perp}(\mathbf{k})$ it is clear that the electron pockets will be much more affected by it than the hole pockets. The bilayer splitting of the electron pocket frequency in the dHvA measurement, if it is to occur, should be smaller or of the order of the half-width at the half-maximum of the peak in the Fourier spectra, otherwise it would have been already resolved.[8,9]
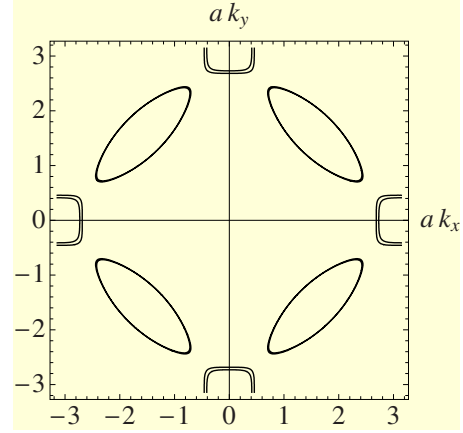

FIG. 7. (Color online) Fermi surface split by bilayer coupling for commensurate DDW. The hole pockets centered at $\frac{1}{2}(\pm\pi/a, \pm\pi/a)$ are essentially unsplit by the bilayer coupling; in contrast, the electron pockets centered at $(\pi/a, 0)$ and symmetry related points are split as described in the text.

Combined with the Luttinger sum rule this provides a strong constraint on the chosen parameters.

As an illustration for $YBa_2Cu_3O_{6.5}$, we choose $t_{\perp} = 8$ meV and $W_0 = 0.0825$ eV, and the chemical potential μ is set to -0.2627 eV, which leads to a hole doping of $n_h \approx 10\%$. The corresponding dHvA frequencies are $F_1 \approx 944$ T, $F_2 \approx 967$ T, $F_3 \approx 570$ T, and $F_4 \approx 450$ T. The frequencies F_1 and F_2, corresponding to the hole pockets are essentially unchanged to our accuracy, while F_3 and F_4 correspond to the electron pockets split by the bilayer coupling. The Fermi surfaces are shown in Fig. 7.

The generalization to the incommensurate case is straightforward and has been discussed previously.[19] Here we do not pursue this further but turn to a number of important conceptual issues.

(1) The interlayer tunneling Hamiltonian is real and cannot lead to orbital currents flowing between the layers. This is actually quite fortunate because the DDW order parameters within the planes remain undistorted. The sole effect of the interlayer Hamiltonian is to lead to linear superpositions of the independent quasiparticle states, which lead to a bilayer splitting, as in a generic two-state system.

(2) If we are to choose opposite phasing of the orbital currents of the two layers and change the matrix to

$$\mathbb{H}' = \begin{pmatrix} \epsilon_{\mathbf{k}} & iW_{\mathbf{k}} & t_{\perp}(\mathbf{k}) & 0 \\ -iW_{\mathbf{k}} & \epsilon_{\mathbf{k}+\mathbf{Q}_0} & 0 & t_{\perp}(\mathbf{k}+\mathbf{Q}_0) \\ t_{\perp}(\mathbf{k}) & 0 & \epsilon_{\mathbf{k}} & -iW_{\mathbf{k}} \\ 0 & t_{\perp}(\mathbf{k}+\mathbf{Q}_0) & iW_{\mathbf{k}} & \epsilon_{\mathbf{k}+\mathbf{Q}_0} \end{pmatrix}, \tag{38}$$

there is no bilayer splitting of the areas of the Fermi pockets. On the other hand, the ground-state energy, to a very high degree of precision, is identical to the previous cases even though the spectra are changed. We suspect that this equality is exact but have not been able to prove it analytically. Therefore, at the level of approximation discussed here, energetics do not allow us to choose between the alternatives

and the correct phasing should be determined from experiments.

(3) We have argued that the interlayer tunneling Hamiltonian is both real and bilinear and therefore does not result in a flow of current between the layers. The only way such currents can appear is if there are further four fermion terms connecting the two layers such as particle-hole or particle-particle pair hopping terms. This would allow us to form further condensates made out of the two layers and would seriously distort the planar DDW order parameter. This has apparently gone unnoticed in Ref. 46. The distortion of DDW order parameter must be thought through anew.

There is a further important consideration that is worth spelling out carefully. One of us recently argued[47] that the first-order interlayer tunneling can be traded by a second-order Hamiltonian in which virtual pair hopping of both particle-particle and particle-hole are present. The second-order Hamiltonian involves four Fermi interactions from which appropriate condensates can be constructed. It was shown there that for such a Hamiltonian antiferromagnetic arrangement of the orbital currents of the layers in a bilayer unit would be lower in energy than the ferromagnetic arrangement. There were two arguments behind this effective Hamiltonian. The first consisted in noticing that the DDW quasiparticle spectra are substantially gapped at the antinodal points. Alas, given the existence of electron pockets in the quantum oscillation experiments, this mechanism could not be operative because there is no longer any gap at the antinodal points. The second argument involved non-Fermi-liquid spectral function. One can easily see that with increased doping there would be Fermi surface reconnections near optimal doping and the electron pockets will evaporate. But at such doping, close to the middle of the superconducting dome, there will be a quantum critical point and one can expect the non-Fermi-liquid behavior.[48] The systematics of the superconducting transition temperature of optimally doped homologous series can still be correctly given by the second-order pair hopping terms.[49]

IV. QUANTUM OSCILLATIONS IN THE MIXED STATE

There is considerable evidence that the quantum oscillation frequencies remain unshifted from the normal state in the mixed state of a wide class of superconductors although there is increased damping arising from vortices.[50] We shall closely follow Stephen[28] where this problem is solved for a conventional metal in the normal state and a s-wave superconductor with a gap Δ_s. Since the Bogoliubov quasiparticles do not couple minimally to the gauge field, they do not form Landau levels and clearly cannot be the source of quantum oscillations.[51] The quantum oscillations must then arise from normal quasiparticles. By solving the Gorkov equations in the mixed state, Stephen arrived at a formula for the self-energy, which for high Landau levels, relevant for the present problem, is

$$\Sigma_n(i\omega) \approx \frac{\Delta_s^2}{\sqrt{4\pi n \hbar \omega_c}} \left[-i\pi \, \mathrm{sgn}(\omega) + \sqrt{\frac{\pi}{n}} \frac{\epsilon_n - \mu}{\hbar \omega_c} \right]. \tag{39}$$

where $\omega_c = \frac{eB}{m^* c}$ and m^* is the corresponding effective mass. The real part of the self-energy shifts the chemical potential

and the Landau-level positions equally. Hence, the real part of the self-energy does not affect the oscillation frequency. The imaginary part of the self-energy leads to the following scattering rate:

$$\frac{\hbar}{\tau_v} = \sqrt{\frac{\pi}{\nu}} \frac{\Delta_s^2}{\hbar \omega_c} = \Delta_s^2 \sqrt{\frac{\pi}{|\mu|\hbar \omega_c}} = \Delta_0^2 \left(1 - \frac{B}{B_{c2}}\right) \sqrt{\frac{\pi}{|\mu|\hbar \omega_c}}, \tag{40}$$

where the filling fraction is $\nu = |\mu|/(\hbar \omega_c)$ and B_{c2} is the upper critical field.

To illustrate our main points, we shall treat the simpler commensurate case. The extension to the incommensurate case is straightforward. There are two cases to consider. The effective mass corresponding to the electron pocket within the commensurate DDW theory, obtained by expanding around $(\pi/a, 0)$, is given by

$$\frac{\hbar^2}{2m^*} \approx \left(2t' + 4t'' - \frac{W_0}{4}\right)a^2. \tag{41}$$

Note that t does not enter in the leading order. Assuming, $W_0 = 0.0825$ eV, $\mu = -0.2642$ eV, and $\Delta_0 = 10$ meV, we get

$$\frac{1}{\tau_v} = 2.9 \times 10^{12} \text{ s}^{-1}, \tag{42}$$

where we have used $B = 40$ T and $B_{c2} = 60$ T for the purpose of illustration. Using Eq. (41) and the parameters given above, we find that $m^* = 1.27 m_e$, where m_e is the free-electron mass.

A more interesting situation arises for the hole pocket, which, to an excellent approximation, can be described by the nodal fermions of DDW. For the purpose of illustration, we choose again the commensurate case. The Stephen formula has to be rederived for nodal fermions.

If the Fermi surface reconstruction is due to SDW, the excitations of both the electron and hole pockets can be approximated by the nonrelativistic Schrödinger equations with the appropriate effective masses and Stephen's formula will apply without further modifications. As an aside, we note that for the spiral SDW given in Ref. 9, the effective masses corresponding to both electron and hole pockets are considerably smaller (of the order of $0.5 m_e$) and do not seem to agree with the experimental results. Similarly, the Dingle factors for the spiral SDW are different from those of the DDW order simply because SDW is gapped everywhere and the excitations are given by nonrelativistic fermions.

A. Commensurate DDW

The linearized two component Hamiltonian for DDW quasiparticles, corresponding to the node $(\pi/2a, \pi/2a)$, in the presence of an external magnetic field is given by

$$H = \int d\mathbf{r} \psi^\dagger(\mathbf{r}) \hat{H}(\mathbf{r}) \psi(\mathbf{r}), \tag{43}$$

where $\psi(\mathbf{r})$ is a two component spinor. The kernel $\hat{H}$ is given by

$$\hat{H} = v_F(p_x - eA_x/c)\sigma_3 + v_D(p_y - eA_y/c)\sigma_2, \quad (44)$$

where σ's are the standard Pauli matrices; v_F is the velocity orthogonal to the Fermi surface, and v_D is the velocity tangential to it; A_x and A_y are the vector potentials and c is the velocity of light. The anisotropy between x and y directions can be removed with the redefinition of the coordinates $\tilde{x} = \sqrt{v_D/v_F}x$ and $\tilde{y} = \sqrt{v_F/v_D}y$. The measure of the integration remains unchanged, as $d\mathbf{r} = d\tilde{\mathbf{r}}$, and $\hat{H}$ becomes

$$\hat{H} = \sqrt{v_F v_D}(p_{\tilde{x}} - eA_{\tilde{x}}/c)\sigma_3 + \sqrt{v_F v_D}(p_{\tilde{y}} - eA_{\tilde{y}}/c)\sigma_2. \quad (45)$$

Under the unitary transformation $\psi \rightarrow U\Psi$, where $U = (1 + i\sigma_2)/\sqrt{2}$, $\hat{H} \rightarrow \hat{H}'$, such that

$$\hat{H}' = \sqrt{v_F v_D}(p_{\tilde{x}} - eA_{\tilde{x}}/c)\sigma_1 + \sqrt{v_F v_D}(p_{\tilde{y}} - eA_{\tilde{y}}/c)\sigma_2. \quad (46)$$

Hence, the energy eigenvalues are

$$\epsilon_{n,\tilde{k},\alpha} = \alpha\sqrt{n}\hbar\tilde{\omega} = \alpha\hbar\sqrt{2nv_F v_D}/l_B, \quad (47)$$

for $n \geq 1$, where $\alpha = \pm 1$ stands for the particle and hole branches of the spectra. Here $\tilde{\omega} = \sqrt{2v_F v_D}/l_B$, $\tilde{k} = 2\pi m/L_{\tilde{y}}$, $m = 0, \pm 1, \pm 2, \ldots$, and the magnetic length $l_B = \sqrt{\hbar c/eB}$. The rescaled length $L_{\tilde{y}} = \sqrt{v_F/v_D}L_y$. For $n = 0$,

$$\epsilon_{0\tilde{k}} = \epsilon_0 = 0. \quad (48)$$

When $\text{sgn}(eB) > 0$, the spinor wave functions in the Landau gauge $\mathbf{A}(\tilde{\mathbf{r}}) = (0, B\tilde{x}, 0)$ are

$$\Psi^{\dagger}_{n \geq 1, \tilde{k}, \alpha}(\tilde{\mathbf{r}}) = \frac{1}{\sqrt{2}}[\varphi^{*}_{n,\tilde{k}}(\tilde{\mathbf{r}}), \alpha\varphi^{*}_{n-1,\tilde{k}}(\tilde{\mathbf{r}})] \quad (49)$$

$$\Psi^{\dagger}_{n=0,\tilde{k}}(\tilde{\mathbf{r}}) = [\varphi^{*}_{0,\tilde{k}}(\tilde{\mathbf{r}}), 0] \quad (50)$$

where

$$\varphi_{n,k}(\tilde{\mathbf{r}}) = \left(\frac{1}{\sqrt{\pi}l_B L_{\tilde{y}} 2^n n!}\right)^{1/2} \exp\left(-i\tilde{k}\tilde{y} - \frac{(\tilde{x} - \tilde{k}l_B^2)^2}{2l_B^2}\right)H_n\left(\frac{\tilde{x} - \tilde{k}l_B^2}{l_B}\right), \quad (51)$$

and H_n are the Hermite polynomials. The matrix Green's function is defined as

$$G_0(\tilde{\mathbf{r}}_1, \tilde{\mathbf{r}}_2, i\omega) = \sum_{n \geq 1, \tilde{k}, \alpha} \frac{\Psi_{n,\tilde{k}}(\tilde{\mathbf{r}}_1)\Psi^{\dagger}_{n,\tilde{k}}(\tilde{\mathbf{r}}_2)}{i\omega - \epsilon_{n,\alpha} + \mu} + \sum_{\tilde{k}} \frac{\Psi_{0,\tilde{k}}(\tilde{\mathbf{r}}_1)\Psi^{\dagger}_{0,\tilde{k}}(\tilde{\mathbf{r}}_2)}{i\omega + \mu}. \quad (52)$$

After performing the sum over $\tilde{k}$ and α, Green's function can be expressed in terms of redefined coordinates as

$$G_0(\tilde{\mathbf{r}}_1, \tilde{\mathbf{r}}_2, i\omega) = \frac{1}{2\pi l_B^2}\exp\left(-\frac{|\tilde{z}_{21}|^2}{4l_B^2}\right)\exp(i\phi_{21})\left[\sum_{n \geq 1}\frac{i\omega + \mu}{(i\omega + \mu)^2 - \epsilon_n^2}\begin{pmatrix} L_n\left(\frac{|\tilde{z}_{21}|^2}{2l_B^2}\right) & 0 \\ 0 & L_{n-1}\left(\frac{|\tilde{z}_{21}|^2}{2l_B^2}\right) \end{pmatrix}\right.$$
$$\left. + \sum_{n \geq 1}\frac{\epsilon_n}{l_B\sqrt{2n}[(i\omega + \mu)^2 - \epsilon_n^2]}\begin{pmatrix} 0 & -\tilde{z}_{21}L^1_{n-1}\left(\frac{|\tilde{z}_{21}|^2}{2l_B^2}\right) \\ \tilde{z}^{*}_{21}L^1_{n-1}\left(\frac{|\tilde{z}_{21}|^2}{2l_B^2}\right) & 0 \end{pmatrix} + \frac{1}{i\omega + \mu}\begin{pmatrix} 1 & 0 \\ 0 & 0 \end{pmatrix}\right], \quad (53)$$

where $\phi_{21} = (\tilde{x}_2 + \tilde{x}_1)(\tilde{y}_2 - \tilde{y}_1)/2l_B^2$, $\tilde{z}_{21} = (\tilde{x}_2 - \tilde{x}_1) + i(\tilde{y}_2 - \tilde{y}_1)$, and L^m_n are the associate Laguerre polynomials. The Gorkov equation for the normal component of Green's function of a s-wave superconductor is

$$G(\tilde{\mathbf{r}}, \tilde{\mathbf{r}}', i\omega) = G_0(\tilde{\mathbf{r}}, \tilde{\mathbf{r}}', i\omega)$$
$$- \int d\tilde{\mathbf{r}}_1 d\tilde{\mathbf{r}}_2 G_0(\tilde{\mathbf{r}}, \tilde{\mathbf{r}}_1, i\omega)\Delta_s(\tilde{\mathbf{r}}_1)G_0(\tilde{\mathbf{r}}_2, \tilde{\mathbf{r}}_1,$$
$$- i\omega)\Delta^{*}_s(\tilde{\mathbf{r}}_2)G_0(\tilde{\mathbf{r}}_2, \tilde{\mathbf{r}}', i\omega), \quad (54)$$

For a disordered configuration of vortices (for other choices, see Stephen[28])

$$V(\tilde{\mathbf{r}}_1, \tilde{\mathbf{r}}_2) = \langle\Delta_s(\tilde{\mathbf{r}}_1)\Delta^{*}_s(\tilde{\mathbf{r}}_2)\exp(2i\phi_{21})\rangle = \Delta_s^2\exp\left(-\frac{(\tilde{\mathbf{r}}_2 - \tilde{\mathbf{r}}_1)^2}{2l_B^2}\right). \quad (55)$$

From the Gorkov equation we can identify the real-space self-energy for the average Green's function to be

$$\Sigma(\tilde{\mathbf{r}}_1, \tilde{\mathbf{r}}_2) = V(\tilde{\mathbf{r}}_1, \tilde{\mathbf{r}}_2)\exp(2i\phi_{21})G_0(\tilde{\mathbf{r}}_2, \tilde{\mathbf{r}}_1, -i\omega). \quad (56)$$

The matrix elements of $\Sigma(\tilde{\mathbf{r}}_1, \tilde{\mathbf{r}}_2)$ in the Landau-level basis are given by

$$\Sigma_{n_1,\tilde{k}_1,\alpha_1;n_2,\tilde{k}_2,\alpha_2}(i\omega)$$

$$= \int d\tilde{\mathbf{r}}_1 d\tilde{\mathbf{r}}_2 \psi^{\dagger}_{n_1,\tilde{k}_1,\alpha_1}(\tilde{\mathbf{r}}_1) V(\tilde{\mathbf{r}}_1,\tilde{\mathbf{r}}_2) \exp(2i\phi_{21}) G_0(\tilde{\mathbf{r}}_2,\tilde{\mathbf{r}}_1,-i\omega)$$

$$\times \psi_{n_2,\tilde{k}_2,\alpha_2}(\tilde{\mathbf{r}}_2). \tag{57}$$

After performing the integrations we obtain

$$\Sigma_{n_1,\tilde{k}_1,\alpha_1;n_2,\tilde{k}_2,\alpha_2}(i\omega) = \frac{\Delta_s^2}{2} \delta_{n_1,n_2} \delta_{\tilde{k}_1,\tilde{k}_2} \left[\sum_{n=0}^{\infty} \frac{(-i\omega+\mu)I_{n_1,n}}{(-i\omega+\mu)^2 - \epsilon_n^2} \right.$$

$$+ \alpha_1\alpha_2 \sum_{n=0}^{\infty} \frac{(-i\omega+\mu)I_{n_1-1,n}}{(-i\omega+\mu)^2 - \epsilon_{n+1}^2} - (\alpha_1$$

$$\left. + \alpha_2)\epsilon_{n_1} \sum_{n=0}^{\infty} \frac{I_{n_1,n}}{(-i\omega+\mu)^2 - \epsilon_{n+1}^2} \right], \tag{58}$$

where

$$I_{n_1,n} = \frac{(n+n_1)!}{n! \, n_1! \, 2^{n+n_1+1}}. \tag{59}$$

When both n and n_1 are large and comparable to the filling fraction $\nu \sim (|\mu|/\hbar\tilde{\omega})^2$,

$$I_{n_1,n} \sim \frac{1}{\sqrt{4\pi n}} \exp\left(-\frac{(n-n_1)^2}{4n}\right) \tag{60}$$

and $\Sigma_n(i\omega) \sim \Sigma_{n_1}(i\omega)$. For large n and n_1, using the asymptotic form of $I_{n_1,n}$, and converting the Landau level sums into integrals we find

$$\Sigma_{n,\alpha_1,\alpha_2}(i\omega) \approx \frac{\Delta_s^2 \mu \sqrt{\pi}}{4\sqrt{n}(\hbar\tilde{\omega})^2} \left\{ \frac{1}{\sqrt{\pi n}} \frac{\mu^2 - \epsilon_n^2}{(\hbar\tilde{\omega})^2} - i \, \text{sgn}(\omega\mu) \right\}$$

$$\times (1-\alpha_1)(1-\alpha_2). \tag{61}$$

It should be noted that for only the hole branch of the spectra is the self-energy nonzero. When $n \sim \nu$, we can neglect the real part of the self-energy and find the vortex contribution to the scattering rate to be

$$\frac{\hbar}{\tau_v} = \sqrt{\frac{\pi}{4}} \frac{\Delta_s^2}{\hbar\tilde{\omega}} = \sqrt{\frac{\pi}{8}} \frac{\Delta_s^2}{\sqrt{|\mu|\hbar\omega_c^*}}, \tag{62}$$

where the effective mass for DDW quasiparticles and the cyclotron frequency analogous to the nonrelativistic case are *defined dimensionally* as

$$m^* = \frac{|\mu|}{v_F v_D}, \tag{63}$$

$$\omega_c^* = \frac{eB}{m^*c}. \tag{64}$$

Note that being relativistic Weyl fermions, there is no real mass associated with them. Here $v_F = 2\sqrt{2}at/\hbar$; to leading order neither t' nor t'' enter. Similarly, $v_D = W_0 a/\sqrt{2}\hbar$. Assuming, again, $\Delta_0 = 10$ meV and $W_0 = 0.0825$ eV, we get

$$\frac{1}{\tau_v} = \frac{28}{\sqrt{B}} \left(1 - \frac{B}{B_{c2}}\right) \times 10^{12} \text{ s}^{-1}, \tag{65}$$

where B is in units of Tesla. For $B = 40$ T and $B_{c2} = 60$ T, we get

$$\frac{1}{\tau_v} = 1.5 \times 10^{12} \text{ s}^{-1}. \tag{66}$$

Despite the relativistic nodal fermionic character of the quasiparticles, the quantum oscillation formulas at zero temperature, using the method of Ando,[52] are formally identical to the nonrelativistic case with appropriate redefinitions. The damped oscillatory factor for the fundamental is[53]

$$e^{-\pi/\omega_c^* \tau_v} \cos(2\pi F/B), \tag{67}$$

where F is again given by the Onsager formula. If we also include the Dingle factor arising from the impurity scattering with a scattering time τ_i, we need to multiply the above formula by a factor $e^{-\pi/\omega_c^* \tau_i}$. At a temperature T, the amplitude, $\mathcal{A}$, is

$$\mathcal{A} \propto \frac{\dfrac{2\pi^2 k_B T}{\hbar\omega_c^*}}{\sinh\left(\dfrac{2\pi^2 k_B T}{\hbar\omega_c^*}\right)}. \tag{68}$$

We emphasize that m^* here is a parameter, not the effective mass of the nodal fermions, which are actually massless. Thus, this formula could not be the conventional Lifshitz-Kosevich formula derived for nonrelativistic fermions, despite its formal similarity. From Eq. (63), the m^* for the parameters given above is $2.72m_e$, more than a factor of 2 larger than the nonrelativistic mass corresponding to the carriers comprising the electron pocket.

If we worked with a d-wave superconductor, then the Gorkov equation is more complicated due to the nonlocal gap function and there will be integration over four variables. However, the final answer for the scattering will not be significantly different from the s-wave answer. We can just replace Δ_s^2 by the Fermi surface averaged $\langle|\Delta_{\mathbf{k}}|^2\rangle$, which is the same as averaging over extremal orbit in 2D.

V. CONCLUSIONS

A. Thoughts on microscopic models

An effective Hamiltonian that can lead to both DDW and d-wave superconductivity (DSC) in Hartree-Fock theory is the following:[54]

$$\mathcal{H} = -\sum_{i,j} t_{ij}(c^{\dagger}_{i\alpha}c_{j\alpha} + \text{H.c.}) - t_c \sum_{\substack{\langle i,j\rangle,\langle i',j\rangle \\ i\neq i'}} c^{\dagger}_{i\alpha}c_{j\alpha}c^{\dagger}_{j\alpha'}c_{i'\alpha'}$$

$$+ U\sum_i n_{i\uparrow}n_{j\downarrow} + V\sum_{\langle i,j\rangle} n_i n_j. \tag{69}$$

In this formula, t_{ij} is hopping matrix element with $t_{ij} = t$ for nearest neighbors, $t_{ij} = -t'$ for next-nearest neighbors, etc.

The operator $n_{i\alpha}$ is the density at a site i and spin α. On the other hand t_c is a correlated hopping term which simultaneously hops an electron from site j to site i and hops an electron from i' into the vacated site j. The on-site and nearest-neighbor repulsions are, respectively, U and V. The repeated spin indices α, α' are assumed to be summed over.

At the mean-field level, the energetics of the DDW order is described by the effective interaction

$$\mathcal{H}_{DDW} = -g_{DDW} \int_{\mathbf{k},\mathbf{k}'} f(\mathbf{k}) f(\mathbf{k}') c^\dagger_{\mathbf{k}+\mathbf{Q}\alpha} c_{\mathbf{k}\alpha} c^\dagger_{\mathbf{k}'\alpha'} c_{\mathbf{k}'+\mathbf{Q}\alpha'}, \tag{70}$$

with $g_{DDW} = 24t_c + 8V$ and $f(\mathbf{k}) = (\cos k_x a - \cos k_y a)$. A similar reduced Hamiltonian for DSC has the coupling $g_{DSC} = 12t_c - 8V$.[54] Note that the processes responsible for both DSC and DDW are essentially kinetic.

A Hamiltonian given in Eq. (69) has a d-wave superconducting ground state over a range of dopings and an antiferromagnetic ground state at half-filling. Since this is the *sine qua non* for any description of the cuprates, we believe that this is a good starting point for further calculations. Correlated hopping terms naturally arise even from the one-band Hubbard model away from half-filling, where their contribution can be computed in t/U perturbation theory

$$t_c \simeq n_h \frac{t^3}{U^2}. \tag{71}$$

At dopings $n_h = 0.1$, for $t/U \sim 0.2$, we would have $g_{DDW} = 2g_{DSC} \sim 0.1t \sim J/2$, J being the antiferromagnetic exchange constant. Thus, not far away from half-filling, correlated hopping terms are certainly not negligible.

Preliminary calculations[55] at the Hartree-Fock level shows that it is difficult to make DDW incommensurate in the relevant underdoped regime. The physical reason is that DDW has nodes. Our mean field results suggest that it costs less energy to dope holes by opening pockets around the nodes rather than by making DDW incommensurate, as long as there is sufficient density of states left at the antinodes to support commensurate DDW. To confirm the above intuition, we tested the effect of gapping the nodes by either introducing s-wave order or including a id_{xy} piece[55] to DDW. We could see that at finite chemical potential, the effect of increasing the nodal gap created by the extra order is to induce a first-order transition to an incommensurate state when the nodal gap amplitude is larger than a critical value of the order of the $d_{x^2-y^2}$ amplitude itself. Of course Hartree-Fock approximation need not be the full answer because the notion of topological doping[56] in the context of stripe order can be equally operative in the present context, a point that requires careful further work.

It is amusing to note that spiral SDW is also generically energetically unfavorable compared to collinear SDW in the weak coupling Hartree-Fock approximation, as was pointed out by Overhauser.[40] The strong-coupling analysis can in principle lead to spirals, but these calculations are difficult to justify.[57]

B. Experimental consequences

If the assumption of incommensurate order is correct we would predict a number of interesting results. First, there should be four frequencies: the electron pocket should be split by the bilayer coupling, although this must be small because otherwise it would have been already resolved. This sets the bilayer splitting in the range of 10–20 meV at the level of 10% doping. In the overdoped regime the experimentally observed bilayer splitting of 88 meV is already known to be substantially smaller than the estimate from the electronic structure calculations, which is about 300 meV.[58] Why bilayer splitting is so small compared to electronic structure calculations is an important theoretical question requiring attention. To satisfy Luttinger sum rule, we not only predict a big hole pocket but also a smaller hole pocket of frequency 250 T. Although there is a very preliminary indication,[9] it needs to be investigated in further measurements and may constitute a confirming evidence of either a spiral SDW or an incommensurate DDW.

IC-DDW could in principle be observed in Y-NMR measurements, as the fact that Y atom is situated at a high-symmetry point is no longer an issue. However, the magnetic field at this site arising from the IC-DDW currents may be too small to observe this splitting.

The most dramatic prediction of IC-DDW is the nonreflection symmetric band structure in a given spin sector. A direct observation of such a band structure will be possible in a spin resolved ARPES measurement. Note that for spiral SDW, up and down spins are mixed. Neutron scattering intensities from such quasiparticle bands may not be sufficient to detect it.

C. Unresolved issues and future directions

On the theoretical side a firm grasp on the existence of IC-DDW is necessary. This is beyond the scope of the present paper whose fundamental concern was to explore the phenomenological consequences of IC-DDW. As it stands, theory seems to favor the commensurate picture, although the predicted hole-pocket in the commensurate case is yet to be observed in quantum oscillation measurements. We expect that many of the experimental puzzles will be resolved in future experiments. It is of course desirable to go beyond Hartree-Fock to formulate a correct microscopic theory of IC-DDW. In particular, diagonal domain walls as a mechanism for incommensuration have not yet been explored. This seems necessary because it seems doubtful that the antiphase-domain walls that result in higher order commensurability, be it from DDW or antiphase spin stripe, can explain the present experiments. Similarly, a rigorous theory of spiral SDW is desirable. As to IC-DDW, it is necessary to go beyond the approximation of retaining only the single harmonic and to formulate a theory that fully conserves currents at the vertices.

The chief experimental puzzle appears to be the conflict of the picture of the Fermi surface emerging from the quantum oscillations with the ARPES measurements.[59,60] Although the hole pocket is not a major concern because it has been argued that the back side of the hole pocket may not be

visible because of the DDW coherence factors[61] and similar coherence factors in other forms of competing mechanism, the nonexistence of the electron pockets is more of a concern. From our previous calculations it is easy to see that at least two sides of the electron pockets should survive the effects of the coherence factors. It is noteworthy that in the past ARPES was able to detect both electron and hole pockets in electron doped cuprates.[62]

Although we do not believe that the observed negative Hall coefficient, its magnitude and oscillations can arise merely from the vortices in the mixed state because it is difficult in such a scenario to obtain multiple Fermi pockets tightly constrained by the Luttinger sum rule, but it would be interesting to explore further the oscillations of the Hall coefficient, in fact it seems almost imperative.

We have argued[19] previously that the ortho-II potential of $YBa_2Cu_3O_{6.5}$ is not an important factor in the explanation of the oscillations in contrast to the discussion in Ref. 46. The highly polarizable BaO-layers next to the chains should screen the potentials quite effectively, to the extent that even disordered chains appear to have little effect in the planar physics in many properties. It is important to recognize that SdH and dHvA (Ref. 63) measurements are also available in $YBa_2Cu_4O_8$ ($\sim$14% doping,[11]) a stoichiometric compound with intrinsic oxygen order, where even the negative Hall coefficient is clearly observed, in agreement with the observations in ortho-II materials.[11] This degree of universality is unachievable if the chain potentials were playing an important role.

A number of competing mechanisms[15,27,64] to explain these unusual experiments have been proposed and discussed in a previous work by one of us.[16] Thus, there is no need to duplicate the discussion here, but the salient questions that must be explained are worth repeating here. Are the oscillations, the negative sign, and the magnitude of the Hall coefficient explainable without invoking a two-band scenario of a hole pocket and an electron pocket? Can the experimentally observed frequencies and the Luttinger sum rule be correctly reproduced? If the spiral spin-density wave order or the antiphase IC-DDW order is the explanation what would be the defining experimental predictions that could be tested in further experiments? If the quasiparticles of a Fermi liquid are truly responsible for the oscillation measurements, what is the role of Mott physics in the cuprates?

The lack of any definitive measurements vindicating the static order parameters necessary to explain Fermi surface reconstruction (recall that dHvA is an equilibrium effect) is worth exploring. A magnetic field even as large as 60 T is not sufficient to provide enough perturbation to energetically nucleate static order in YBCO with an order parameter large enough to reproduce the measurements, especially in $YBa_2Cu_4O_8$ with about 14% doping. We hope that as other cuprates are explored and the theoretical tools are sharpened, many of these questions will be answered and will provide a resolution of the enigma of high T_c.

[1] S. Chakravarty, B. I. Halperin, and D. R. Nelson, Phys. Rev. B **39**, 2344 (1989).

[2] S. A. Kivelson, I. P. Bindloss, E. Fradkin, V. Oganesyan, J. M. Tranquada, A. Kapitulnik, and C. Howald, Rev. Mod. Phys. **75**, 1201 (2003).

[3] S. A. Kivelson, E. Fradkin, and V. J. Emery, Nature (London) **393**, 550 (1998).

[4] C. M. Varma, Phys. Rev. Lett. **83**, 3538 (1999).

[5] S. Chakravarty, R. B. Laughlin, D. K. Morr, and C. Nayak, Phys. Rev. B **63**, 094503 (2001).

[6] S. Caprara, C. Castellani, C. di Castro, M. Grilli, and A. Sadori, J. Phys. IV **9**, Pr10-329 (1999).

[7] S.-C. Zhang, Science **275**, 1089 (1997).

[8] C. Jaudet *et al.*, Phys. Rev. Lett. **100**, 187005 (2008).

[9] S. E. Sebastian, N. Harrison, E. Palm, T. P. Murphy, C. H. Mielke, R. Liang, D. A. Bonn, W. N. Hardy, and G. G. Lonzarich, Nature (London) **454**, 200 (2008).

[10] E. A. Yelland, J. Singleton, C. H. Mielke, N. Harrison, F. F. Balakirev, B. Dabrowski, and J. R. Cooper, Phys. Rev. Lett. **100**, 047003 (2008).

[11] D. LeBoeuf *et al.*, Nature (London) **450**, 533 (2007).

[12] N. Doiron-Leyraud, C. Proust, D. LeBoeuf, J. Levallois, J.-B. Bonnemaison, R. Liang, D. A. Bonn, W. N. Hardy, and L. Taillefer, Nature (London) **447**, 565 (2007).

[13] A. F. Bangura *et al.*, Phys. Rev. Lett. **100**, 047004 (2008).

[14] S. Chakravarty, Science **319**, 735 (2008).

[15] P. A. Lee, Rep. Prog. Phys. **71**, 012501 (2008).

[16] S. Chakravarty and H.-Y. Kee, Proc. Natl. Acad. Sci. U.S.A. **105**, 8835 (2008).

[17] P. W. Anderson, Science **235**, 1196 (1987).

[18] B. I. Halperin and T. M. Rice, in *Solid State Physics*, edited by F. Seitz and D. Turnbull (Academic, San Diego, 1968), p. 115.

[19] X. Jia, I. Dimov, P. Goswami, and S. Chakravarty, arXiv:0806.3793 (unpublished).

[20] A. Kopp, A. Ghosal, and S. Chakravarty, Proc. Natl. Acad. Sci. U.S.A. **104**, 6123 (2007).

[21] U. Schollwöck, S. Chakravarty, J. O. Fjærestad, J. B. Marston, and M. Troyer, Phys. Rev. Lett. **90**, 186401 (2003).

[22] V. J. Emery, S. A. Kivelson, and J. M. Tranquada, Proc. Natl. Acad. Sci. U.S.A. **96**, 8814 (1999).

[23] C. Stock, W. J. L. Buyers, Z. Tun, R. Liang, D. Peets, D. Bonn, W. N. Hardy, and L. Taillefer, Phys. Rev. B **66**, 024505 (2002).

[24] B. Fauqué, Y. Sidis, V. Hinkov, S. Pailhes, C. T. Lin, X. Chaud, and P. Bourges, Phys. Rev. Lett. **96**, 197001 (2006).

[25] H. A. Mook, P. Dai, S. M. Hayden, A. Hiess, J. W. Lynn, S. H. Lee, and F. Doğan, Phys. Rev. B **66**, 144513 (2002).

[26] H. A. Mook, P. Dai, S. M. Hayden, A. Hiess, S. H. Lee, and F. Doğan, Phys. Rev. B **69**, 134509 (2004).

[27] A. J. Millis and M. R. Norman, Phys. Rev. B **76**, 220503(R) (2007).

[28] M. J. Stephen, Phys. Rev. B **45**, 5481 (1992).

[29] C. Nayak, Phys. Rev. B **62**, 4880 (2000).

[30] J. B. Marston and I. Affleck, Phys. Rev. B **39**, 11538 (1989).

[31] A. A. Nersesyan, G. I. Japaridze, and I. G. Kimeridze, J. Phys.: Condens. Matter **3**, 3353 (1991).

[32] S. Chakravarty, Phys. Rev. B **66**, 224505 (2002).

[33] H. J. Schulz, Phys. Rev. Lett. **64**, 1445 (1990).

[34] H. J. Schulz, J. Phys. (Paris) **50**, 2833 (1989).

[35] O. K. Andersen, A. I. Liechtenstein, O. Jepsen, and F. Paulsen, J. Phys. Chem. Solids **56**, 1573 (1995).

[36] A. Damascelli, Z. Hussain, and Z.-X. Shen, Rev. Mod. Phys. **75**, 473 (2003).

[37] P. Dai, H. A. Mook, R. D. Hunt, and F. Doğan, Phys. Rev. B **63**, 054525 (2001).

[38] G. E. Volovik, *The Universe in a Helium Droplet* (Cambridge University Press, Cambridge, 2003).

[39] I. Dzyaloshinskii, Phys. Rev. B **68**, 085113 (2003).

[40] A. W. Overhauser, Phys. Rev. **128**, 1437 (1962).

[41] L. L. Daemen and A. W. Overhauser, Phys. Rev. B **39**, 6431 (1989).

[42] H.-Y. Kee and Y. B. Kim, Phys. Rev. B **66**, 012505 (2002).

[43] J. Lin and A. J. Millis, Phys. Rev. B **78**, 115108 (2008).

[44] L. M. Falicov and M. J. Zuckermann, Phys. Rev. **160**, 372 (1967).

[45] S. Chakravarty, A. Sudbø, P. W. Anderson, and S. Strong, Science **261**, 337 (1993).

[46] D. Podolsky and H.-Y. Kee, arXiv:0806.0005 (unpublished).

[47] A. Kopp and S. Chakravarty, Proc. SPIE **5932**, 593219 (2005).

[48] R. Daou *et al.*, arXiv:0806.2881 (unpublished).

[49] S. Chakravarty, H. Y. Kee, and K. Völker, Nature (London) **428**, 53 (2004).

[50] A. Wasserman and M. Springford, Adv. Phys. **45**, 471 (1996).

[51] M. Franz and Z. Tešanović, Phys. Rev. Lett. **84**, 554 (2000).

[52] T. Ando, J. Phys. Soc. Jpn. **37**, 1233 (1974).

[53] P. Goswami and S. Chakravarty (unpublished).

[54] C. Nayak and E. Pivovarov, Phys. Rev. B **66**, 064508 (2002).

[55] I. Dimov, Ph.D. thesis, University of California Los Angeles, 2008; arXiv:cond-mat/0512627 (unpublished).

[56] L. P. Pryadko, S. A. Kivelson, V. J. Emery, Y. B. Bazaliy, and E. A. Demler, Phys. Rev. B **60**, 7541 (1999).

[57] B. I. Shraiman and E. D. Siggia, Phys. Rev. Lett. **62**, 1564 (1989).

[58] D. L. Feng *et al.*, Phys. Rev. Lett. **86**, 5550 (2001).

[59] M. A. Hossain *et al.*, Nat. Phys. **4**, 527 (2008).

[60] J. Chang *et al.*, New J. Phys. **10**, 103016 (2008).

[61] S. Chakravarty, C. Nayak, and S. Tewari, Phys. Rev. B **68**, 100504(R) (2003).

[62] N. P. Armitage *et al.*, Phys. Rev. Lett. **87**, 147003 (2001).

[63] B. Vignolle, A. Carrington, R. A. Cooper, M. M. J. French, A. P. Mackenzie, C. Jaudet, D. Vignolles, Cyril Proust, and N. E. Hussey, Nature (London) **455**, 952 (2008).

[64] W. Q. Chen, K. Y. Yang, T. M. Rice, and F. C. Zhang, Europhys. Lett. **82**, 17004 (2008).